Hindawi Publishing Corporation
Journal of Chemistry
Volume 2013, Article ID 965041, 12 pages
http://dx.doi.org/10.1155/2013/965041

Research Article

Biosorption Behavior of Basic Red 46 and Violet 3 by Dead *Pleurotus mutilus* from Single- and Multicomponent Systems

N. Yeddou Mezenner,[1] A. Hamadi,[1] S. Kaddour,[2] Z. Bensaadi,[1] and A. Bensmaili[1]

[1] *Laboratory of Chemical Engineering, Faculty of Mechanical and Chemical Engineering, University of Sciences and Technology Houari-Boumediene, USTHB, BP 32 El Alia, Bab Ezzouar, Algiers, 16111, Algeria*
[2] *Faculty of Chemistry, University of Sciences and Technology Houari-Boumediene, USTHB, BP 32 El Alia, Bab Ezzouar, Algiers, 16111, Algeria*

Correspondence should be addressed to N. Yeddou Mezenner; yeddouna@yahoo.fr

Received 26 June 2012; Revised 24 September 2012; Accepted 25 September 2012

Academic Editor: Hassan Arida

The performance of nonviable *P. mutilus* for removal of Crystal Violet (CV) and Basic Red 46 (BR46) was investigated in single and binary systems. Batch kinetic studies were carried out as a function of pH, temperature, biomass amount, and dye concentration to determine the decolorization efficiency of biosorbent. In single system, the biosorption capacities of *P. M.* reached 166 and 76.92 mg/g for CV and BR46, respectively. A comparison of kinetic models applied to the adsorption of basic dyes onto *P. Mutilus* was evaluated for the pseudo-second-order and intraparticle diffusion kinetics models. The experimental data fitted very well the pseudo-second-order kinetic model, whereas diffusion is not only the rate-controlling step. The thermodynamic study indicates that the adsorption of dyes is spontaneous and endothermic process. In binary system, the biosorption capacities of *P. Mutilus* for both dyes decreased significantly compared to that in single system. Competitive coefficients calculated on a concentration basis using Sheindorf-Rebhun-Sheintuch (SRS) equation were useful for describing the degree of competitive interaction in *P. M.*

1. Introduction

The release of synthetic dyestuffs into the aquatic ecosystems through the wastewater of textile industries is a global environmental concern [1]. The immense volume of aromatic structures present in dye molecules makes wastewater treatment through a biological process ineffective. As a result, the removal of dyes from wastewater is important for the environmental protection and human health. To avoid the ecological health problems, many methods were developed for removing dyes.

Biosorption is one of the popular and attractive technologies for the removal of color contaminants from aqueous effluents. Biosorption is a process that utilizes inexpensive dead biomass to sequester inorganic [2–9] and organic ions [10–13]. It has retained a great attention for the last decades as an alternative to conventional processes (such as membrane processes, ion exchange, etc.) for the removal of dye from aqueous solutions, therefore, a wide variety of microorganisms including bacteria, fungi, and yeasts are used for the biosorption of a broad range of dyes [14–16]. Much of the work on the biosorption of dyes by various kinds of biosorbents has focused on the uptake of single dyes [17–21] but fewer studies were conducted to investigate adsorption behavior of biosorbent for dyes in multicomponent systems. In practice, most industrial effluents contain a mixture of several dyes, thus, it is necessary to study the simultaneous biosorption of two or more dyes from aqueous solutions.

A variety of biomasses is used by the SAIDAL antibiotic complex at Medea, (Algeria) among which the basidomycete *Pleurotus mutilus* from which an antibiotic (pleuromutilin) for veterinary use, is isolated. Our previous study [22] explored the feasibility of utilizing *Pleurotus mutilus* as biosorbent for Basic Blue 41 removal from aqueous solution in single system. At present, this study aims: (i) to investigate the biosorption of basic violet 3 and Basic Red 46, currently used in Algeria onto dead *Pleurotus mutilus* in single and bicomponent systems in different concentration

ratios, and to (ii) model the experimental results using the SRS equation. In doing so, the biosorption of basic dyes on this waste material from aqueous solutions was evaluated in batch experiments. The adsorption isotherms, kinetics, and temperature effect were studied.

2. Materials and Methods

2.1. Dyes and Analysis. The sorbates used in the experiments were Basic red 46 (BR46) and Crystal violet (CV) or genetian violet which are used in textile processing Industry of Algier (Algeria). These dyes are suitable for dyeing of acrylic substrates, some polyamide and polyester types, viscose, cotton, and wool. CV is also used as an active ingredient in Gram's stain and as a bacteriostatic agent in animal husbandry and veterinary practice [23, 24]. The chemical structures of these dyes are shown in Figure S1 (Supplementary data available online at doi:10.1155/2013/965041). A stock of aqueous solution of the dyes was prepared in deionised water in the concentration of 1000 mg/L.

Batch kinetic biosorption studies were conducted in a temperature-controlled stirrer using 1000 mL of adsorbate solution. Samples were withdrawn at suitable intervals and were separated from the sorbent by centrifugation for 20 min at 5000 rpm and then analyzed using a UV spectrophotometer.

For the single system, the dye concentrations were determinated by measuring the absorbance at wavelength of maximum absorbance of CV (594 nm), and BR46 (530 nm) and then calculated according to the calibration curves, respectively.

For components of a binary system, the concentrations of each dye in mixture solutions can be computed using (1) [29]

$$C_{\mathrm{BR46}} = \frac{K_{\mathrm{CV2}} d_{\lambda 1} - K_{\mathrm{CV1}} d_{\lambda 2}}{K_{\mathrm{BR}_{461}} K_{\mathrm{CV2}} - K_{\mathrm{BR}_{462}} K_{\mathrm{CV1}}},$$
$$C_{\mathrm{BR46}} = \frac{K_{\mathrm{BR}_{461}} d_{\lambda 2} - K_{\mathrm{BR}_{462d1}}}{K_{\mathrm{BR}_{461}} K_{\mathrm{CV2}} - K_{\mathrm{BR}_{462}} K_{\mathrm{CV1}}}, \quad (1)$$

where 1 and 2 represent components in a binary system. $K_{\mathrm{BR461}}, K_{\mathrm{CV1}}, K_{\mathrm{BR461}}$, and K_{CV2} are the calibration constants for components 1 and 2 at λ_1 and λ_2, respectively, d_1 and d_1 are the optical densities at λ_1 and λ_2, respectively.

2.2. Biomass Preparation. Waste *P. mutilus* biomass was collected at the SAIDAL antibiotic production complex at Medea (Algeria). The collected samples were washed repeatedly with deionised water to remove extraneous materials and salts and dried for 24 h at 50°C in an oven. The dried biomass was ground manually in a mortar and sieved into particle size ranges: 110–215 μm.

2.3. Sorption Isotherms. Adsorption experiments were carried out by adding a fixed amount of adsorbent (0.6 and 0.7 g/L for CV and BR46, resp.) to a series of conical flasks filled with 100 mL diluted solutions (10–120 mg/L). The conical flasks were placed in a thermostatic shaker at 10, 15, 20, and 30° at pH 7.5. The removal efficiency (E) of dye on *P. M.* and sorption capacity, (q) were calculated from (2):

$$E\,(\%) = \frac{C_i - C_f}{C_i} \times 100,$$
$$q = \frac{V\left(C_i - C_f\right)}{m}. \quad (2)$$

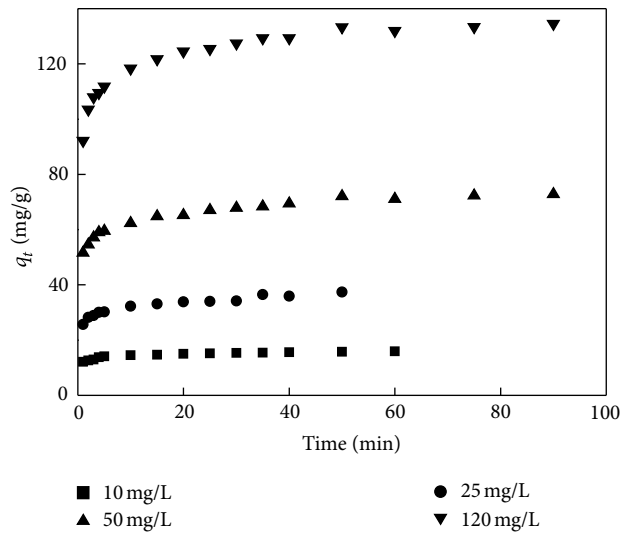

Figure 1: Effect of contact time at several initial CV concentrations on sorption kinetics (30°C, pH 7, C_s = 0.6 g/L).

3. Results and Discussion

3.1. Biosorption in Single Dye

3.1.1. Effect of Initial Dye Concentration and Contact Time. Experiments were undertaken to study the effect of varying initial concentration (10–120 mg/L) at 30°C on dye removal by dead *P. mutilus*. Figures 1 and 2 represent the effect of initial dye concentration on the biosorption on *P. M* for CV and BR46 at pH 7.5 and 8.1, respectively. The rate of dye uptake is found to be very rapid during the initial 5 min, and thereafter, the rate of dye ions uptake decreases considerably. No significant change in dye uptake is observed after about 25 min. Initially, the surface of *P. M.* was vacant, and the biosorption rate was fast.

After a lapse of some time, the remaining vacant surface sites are difficult to be occupied due to repulsive forces between the adsorbate on the *P. M.* surface and in the bulk phase. An increase in initial dye concentration led to an increase in the biosorption capacity of dye on *P. M.*, and longer time was required to reach equilibrium. The data showed that as the initial concentration of the dye increased from 10 to 120 mg/L the biosorption capacity increased from 10.76 to 49.89 mg/L for BR46 and from 15.94 to 134.53 mg/L for CV. This showed that biosorption capacity was highly concentration dependent. Also, it was found that the values of q_e for CV were greater than that for BR46 at any C_i.

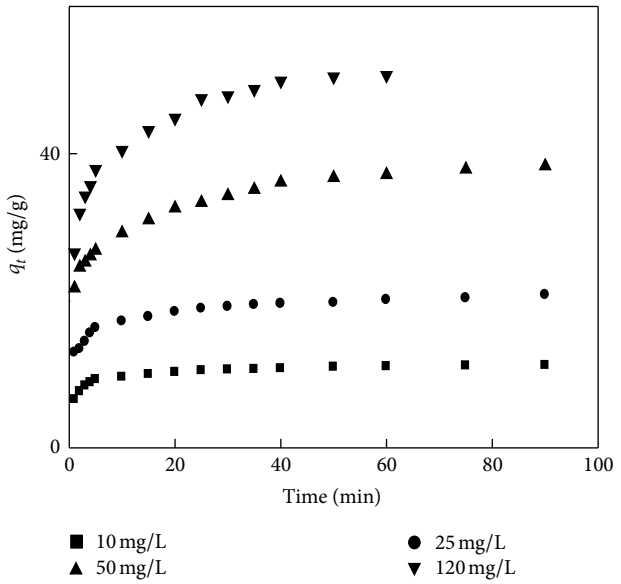

Figure 2: Effect of contact time at several initial BR46 concentrations on sorption kinetics (30°C, pH 7, C_s = 0.7 g/L).

3.1.2. Effect of Biosorbent Concentration. The sorbent concentration is another factor that influences the sorption equilibrium. In order to examine the effect of the sorbent dosage on the removal efficiency dye, adsorption experiments were set up with various amounts of dried *P. M.* (0.2, 0.4, 0.6, 0.7, and 0.8 g/L) and dye concentrations (10 mg/L). During the adsorption, the temperature of system was kept constant at 30°C. The effect of sorbent dosages on the percentage removal of both dyes is shown in Figure 3.

It followed the predicted pattern of increasing percentage sorption as the dosage was increased and reaches a saturation level at high doses, 0.6 and 0.7 g/L of biosorbent were observed to be the upper limit for the removal of CV and BR46 respectively. This is probably because of the resistance to mass transfer of dye from bulk liquid to the surface of the solid, which becomes important at high-adsorbent loading in the conical flask in which the experiment was conducted.

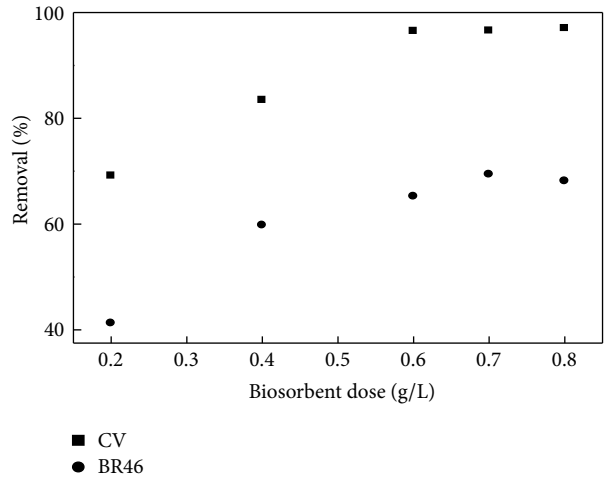

Figure 3: Effect of biosorbent dosage on BR46 and CV removal.

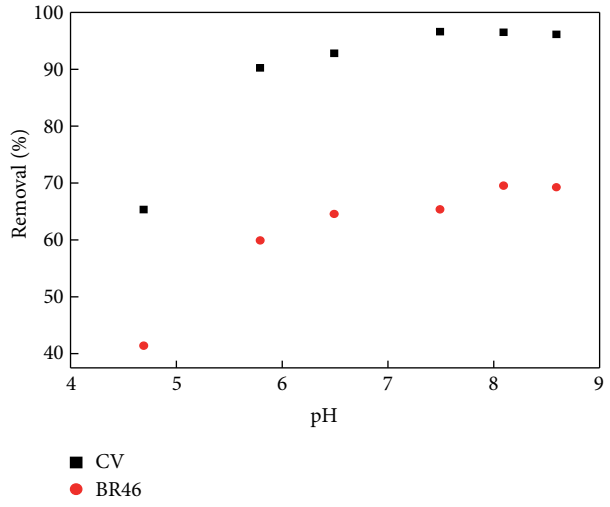

Figure 4: Effect of pH on BR46 and CV removal.

3.1.3. Effect of pH. Adsorption equilibrium studies were conducted at initial dye concentration of 50 mg/L by adding a fixed amount of adsorbent (0.6 g and 0.7 g for CV and BR46, resp.) into a series of conical flasks each filled with 1000 mL of dye solution. Batch sorption experiments were performed at various aqueous phase pH (4.7, 5.8, 6.5, 7.5, 8.1, and 8.6). During the adsorption, the temperature of system was kept constant at 30°C.

The pH of the dye solution plays an important role in the whole biosorption process and particularly in the adsorption capacity, influencing the surface charge of the biosorbent, the degree of ionization of the dye present in the solution and the dissociation of functional groups on the active sites of biosorbent, and the solution dye chemistries. The fungal cell wall contains a high amount of polysaccharides and some of them are associated with proteins and other components. These macromolecules have several functional groups, and the biosorption phenomenon depends on the protonation or unprotonation of these functional groups on the surface of the cell wall [30]. Figure 4 indicates the removal of dye by dead *P. mutilus* at various initial pH values ranging from 4.7 to 8.6 in 10 mg/L of dye solution. Evidently pH significantly affected the extent of adsorption of dye.

The results of percentage of dye removal versus equilibrium pH increased with increasing pH. Further the variation in pH (7.5–8.6) did not cause any disintegration of the biosorbent, and the extent of adsorption was observed to become nearly constant at pH values greater than 7.5. As the initial pH of the dye solution decreased, the number of negatively charged adsorbent sites decreased and positively

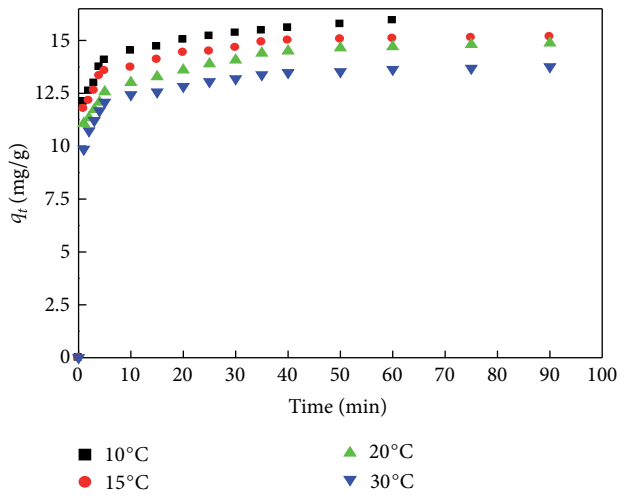

Figure 5: CV adsorption on *P. Mutilus* at various temperatures (C_0 = 10 mg/L, pH 7, C_s = 0.7 g/L).

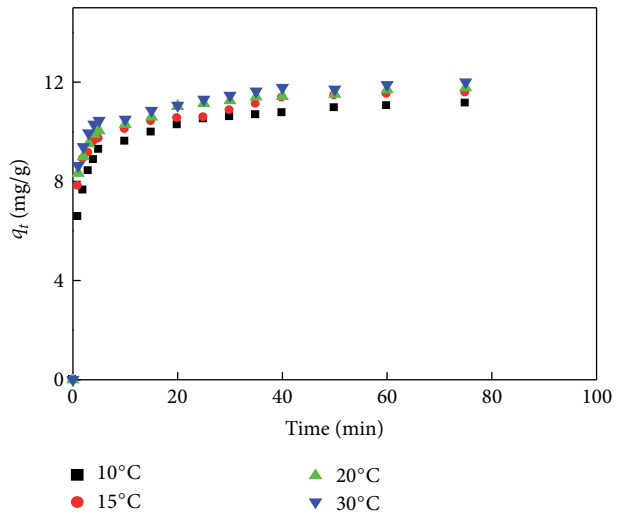

Figure 6: BR46 adsorption on *P. Mutilus* at various temperatures (C_0 = 10 mg/L, pH 7, C_s = 0.7 g/L).

charged sites increased which did not favor the adsorption of positively charged dye cation due to electrostatic repulsion [31].

The lower uptake of dye adsorption at acidic pH is also due to the presence of excess of H^+ ions competing with dye cation for the adsorption sites. Therefore, ionic exchange, electrostatic repulsion, structural properties of the dye and *pleurotus Mutilus* biomass could play a vital role in dye adsorption processes using fungal biomass.

All the two dyes found to follow the similar trend with low percentage of removal at low pH (pH = 4.7). At pH 7.5 and 8.1, the maximum adsorption onto *P. M.* for 10 mg/L initial dye concentration was 96.48% for CV and 69.4% for BR46 respectively.

There were many factors responsible for this difference in dye uptake, such as their structure, molecular size, and functional groups.

3.1.4. Effect of Temperature. The effect of temperature on BR46 and CV uptake capacity (q_e) of *P. M.* was studied. From Figures 5 and 6, it was observed that the BR46 and CV uptake capacity (q_e) of *P. M.* increased with increasing temperature up to 30°C, indicating that the adsorption of BR46 and CV ions was favored at higher temperatures. Increase of q_e with increasing temperature might be due to the increase of kinetic energy of the dye in solution, which increased the collision rate with the surface of the adsorbent [32]. Also the increase in adsorption with temperature may be attributed to either increase in the number of active surface sites available for adsorption on the *P. M.* or the decrease in the thickness of the boundary layer surrounding the *P. M.*. It means that the sorption of BR46 and CV is endothermic.

3.2. Modelling of the Sorption Equilibrium Depending Temperature. In order to optimize the design of a sorption system to remove dyes from aqueous solutions, it is important to establish the most appropriate correlation for the equilibrium curves. The isotherms data were analyzed using two of the most commonly used equilibrium models, Langmuir [33] and Freundlich [34]. The mathematical expressions are given by (3), respectively, as follows:

$$q_e = q_{\max}\frac{bC_e}{1+bC_e}, \qquad q_e = K_f \cdot C_e^{1/n}, \tag{3}$$

where $q_{\max}$ (mg/g), is the maximum amount of sorbate per unit weight of adsorbent, to form a complete monolayer on the surface bound at high C_e and b (L/mg) is a constant related to the affinity of the binding sites. $q_{\max}$ and b can be determined from the linear plot of C_e/q_e versus C_e. K_f and n are the Freundlich constants characteristics of the system ($n$dimensionless; K_f (mg$L^{-1/n}$ g^{-1} $L^{1/n}$)). Equation (6) can be linearized in logarithmic form and the Freundlich constants can then be determined.

The effects of temperature on biosorption were studied at initial dye concentration (10 mg/L), fixed initial pH (7.5 and 8.1 for CV and BR46, resp.) and biomass concentration (0.6 and 0.7 g/L for CV and BR46, resp.) for 90 min. Adsorption isotherms in single-component systems are presented in Figures 7, 8, 9, and 10. With increasing temperature from 10 to 30°C, $q_{\max}$ increases from 71.43 to 166.66 mg/g and from 62.5 to 76.92 mg/g for CV and BR46, respectively. The best-fit values of the model parameters estimated from (3) and (6) by linear regression analyses are listed in Table 1. Also shown are the correlation coefficients (r^2), which provide measure of model fitness. A comparison of the experimental isotherms with the adsorption isotherm models showed that

Table 1: Biosorption isotherm parameters for the biosorption of CV and BR46 onto *P. Mutilus* in single system at various temperatures.

Parameters	Temperature			
	10°C	15°C	20°C	30°C
		BR46		
Freundlich constants				
n	2.18	2.25	2.47	2.60
K_f (mg $L^{-1/n} g^{-1} L^{1/n}$)	6.38	7.47	9.50	10.91
r^2	0.99	0.983	0.995	0.996
Langmuir constants				
q_{max} (mg/g)	62.5	66.66	71.43	76.92
b (L/mg)	0.046	0.054	0.06	0.065
r^2	0.98	0.977	0.963	0.959
		CV		
Freundlich				
n	2.82	2.77	2.38	2.35
K_f (mg $L^{-1/n} g^{-1} L^{1/n}$)	11.26	13	19	22.35
r^2	0.96	0.97	0.96	0.986
Langmuir				
q_{max} (mg/g)	71.43	90.91	142.85	166.66
b (L/mg)	0.058	0.054	0.0625	0.089
r^2	0.932	0.907	0.829	0.934

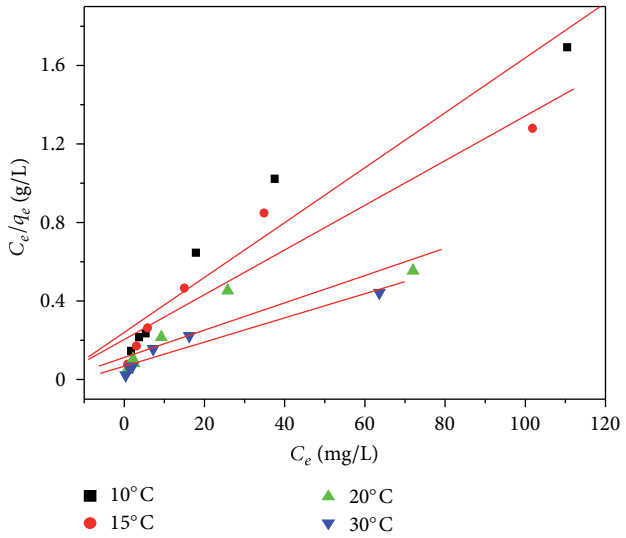

Figure 7: Langmuir adsorption isotherm for CV on *P. Mutilus* at various temperatures.

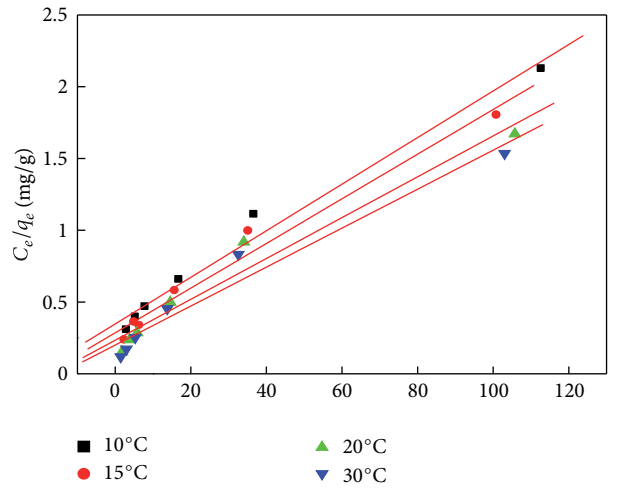

Figure 8: Langmuir adsorption isotherm for BR46 on *P. Mutilus* at various temperatures.

the Langmuir equation represented the poorest fit of experimental data as compared to the Freundlich isotherm. The equilibrium adsorption data for CV and BR46 biosorption on *P. M.* can be represented appropriately by Freundlich model in the studied concentration and temperature range. It is found from Table 1 that the *P. M.* shows greater heterogeneity for CV than that for BR46 ions. Since $n > 1$; both the dye ions are favourably adsorbed by *P. M.*. The K_f values indicate the higher uptake of CV (K_f = 22.35 mg $L^{-1/n}$ g^{-1} $L^{1/n}$ at T = 30°C) than that of BR46 ions (K_f = 10.91 mg $L^{-1/n}$ g^{-1} $L^{1/n}$ at T = 30°C) by *P. M.*.

3.3. Biosorption Kinetics

3.3.1. Kinetic Models. The studies of adsorption equilibrium are important in determining the effectiveness of adsorption; however, it is also necessary to identify the types of adsorption mechanism in a given system.

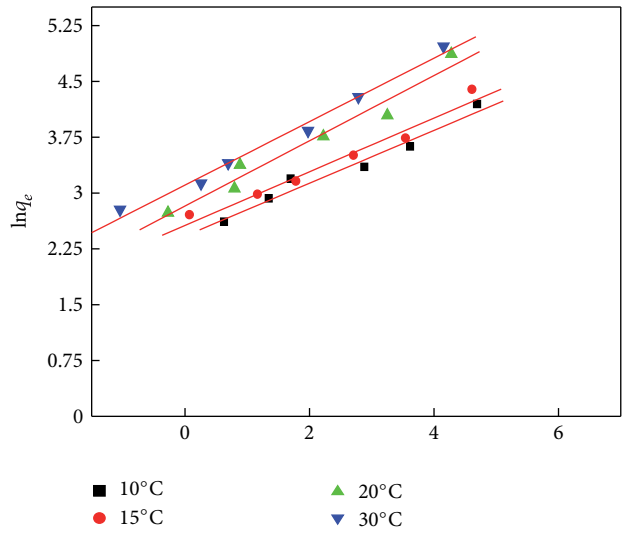

Figure 9: Freundlich adsorption isotherm for CV on *P. Mutilus* at various temperatures.

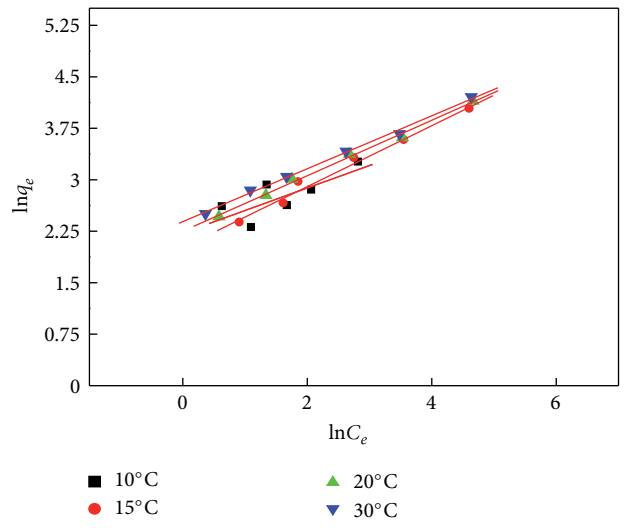

Figure 10: Freundlich adsorption isotherm for BR46 on *P. Mutilus* at various temperatures.

The kinetic of biosorption of CV and BR46 had been modeled using (4)–(7) given below.

Pseudo-second order

$$\frac{t}{q_t} = \frac{1}{k_2 \cdot q_e^2} + \frac{t}{q_e} \tag{4}$$

$$h = k_2 q_e^2 \tag{5}$$

see [25].

Intraparticle diffusion

$$q_t = k_i t^{1/2} + C \tag{6}$$

see [26, 27].

Pore diffusion coefficient

$$D_p = \frac{0.03xr^2}{t_{1/2}} \tag{7}$$

see [28],

where q_t and q_e are adsorption capacities (mg/g) at any time, t (min) and equilibrium, respectively; K_2 (g·/mg/min), h (mg/g.min), K_i (g/mg·min$^{0.5}$), Di (cm^2/s), $t_{1/2}$(s) and r(cm), the rate constant of pseudo-second-order adsorption, initial adsorption rate, intraparticle diffusion rate constants, diffusion coefficient, time for half-adsorption of dye, and the average radius of the adsorbent particle, respectively. The value of r (average radius) was calculated as 67×10^{-4} cm. In these calculations, it has been assumed that the solid phase consists of spherical particles.

Pseudo Second Order. The application of the linear form of pseudo-second-order kinetic model on our experimental results is presented in Figures (S2–S5) (Supplementary data). Both constants K_2 and h were calculated from the intercept and slope of the line obtained by plotting t/q_t versus t. It can be seen from Table 2 that the kinetics of BR46 and CV adsorption onto *P. M.* follow this model with correlation coefficients higher than 0.999 and the equilibrium adsorption capacity, q_e, increases as the initial dye concentration, C_i, increases from 10 to 120 mg/L. Further, it was found that the variations of the rate constant, K_2, seem to have a decreasing trend with increasing initial dye concentration for both dyes. The variations of t/q_t versus t at various temperatures of the dye solution under the initial concentration of 10 mg/L still confirmed to fit the pseudo-second-order model. The values of model parameters (K_2, h,and q_e) for different temperatures have been calculated from (4) and (5), and the results are given in Table 2, revealing that the fitted adsorption capacity of both dyes on *P. M.* at equilibrium, q_e, increased with increasing temperature. Thus, on increasing the solution temperature from 10 to 30°C, the value of q_e increased from 13.89 to 16.13 mg/g and from 11.36 to 12.05 mg/g for CV and BR46, respectively Also, from Table 2, it was noticed that the initial adsorption rate, h, increases with increasing temperature. These results imply that chemisorption mechanism may play an important role.

Intraparticle Diffusion Model. The pseudo-second-order model could not identify the diffusion mechanism, and the kinetic results were then analyzed by using the intraparticle diffusion model. In the model developed by Weber and Morris [26], McKay and Poots [27], the initial rate of intraparticle diffusion is calculated by linearization of (6).

According to this model, the plot of uptake, q_t, versus the square root of time ($t_{1/2}$) should be linear if intraparticle diffusion is involved in the adsorption process and if these lines pass through the origin then intra-particle diffusion is the rate-controlling step [35]. When the plots do not

pass through the origin, this is indicative of some degree of boundary layer control and this further shows that the intra-particle diffusion is not the only rate-limiting step, but also other kinetic models may control the rate of adsorption, all of which may be operating simultaneously [36]. From Figures (S6–S9), it can be observed that the straight lines did not pass through the origin and this further indicates that the intra-particle diffusion is not the only rate-controlling step. The intra-particle diffusion, K_i, values were obtained from the slope of the straight line portions of plot of q_t versus $t_{1/2}$ for various dye concentrations and solutions temperature (Figures S6–S9). The correlation coefficients (r^2) of the intra-particle diffusion model are given in Table 2; they are lower than that of the pseudo-second-order kinetic model. This suggests that the BR46 and CV biosorption process appears to be controlled by the chemical reaction. It was observed that intra-particle rate constant values (K_i) increased with initial dye concentration. The observed increase in K_i values with increasing initial dye concentration can be explained by the growing effect of driving force resulted in reducing the diffusion of dye in the boundary layer and enhancing the diffusion in the solid. Also, as shown in Table 2, increasing the temperature promoted the pore diffusion in sorbent particles and resulted in an enhancement in the intra-particle diffusion rate [37]. The corresponding values of intraparticle diffusion rate constant, K_i, for the various concentrations of CV and BR46 (10–120 mg/L) varied from 0.522 to 4.31 mg/g $\text{min}^{1/2}$ and from 0.453 to 3.35 mg/g $\text{min}^{1/2}$, respectively (Table 2). It is found from Table 2 that the rate parameters of CV are greatly bigger than BR46 and that may be due to the difference in the molecule structures of both dyes.

Diffusion Coefficient. The diffusion coefficients for the intraparticle transport of CV and BR46 within the pores of *P. M.* particles have been calculated at different initial dye concentrations and temperatures by using (7). The values of diffusion coefficient for biosorption of CV and BR46 increase from 2.81×10^{-8} to $3.29 \times 10^{-8}\,\text{cm}^2/\text{s}$ and from 2.03×10^{-8} to 2.54×10^{-8} with change in temperature from 10 to 30°C. Based on Table 2, the results are comparable to those published in literature.

3.3.2. Thermodynamic Study. The thermodynamic parameters of the adsorption process were determined from the experimental data obtained using the following equations [38]:

$$\Delta G^\circ = -RT\,LnK_d,$$
$$LnK_d = -\frac{\Delta H^\circ}{RT} + \frac{\Delta S^\circ}{R}, \tag{8}$$

where K_d is the distribution coefficient for the adsorption, ΔS°, ΔH° and ΔG° are the change of entropy, enthalpy and the Gibbs energy, T is the absolute temperature, R is the gas constant.

Figure 11 shows a linear relationship between the logarithm of rate constant and the reciprocal of temperature. The values of $\Delta H^\circ$and ΔS° were determined from the slope and intercept of the plot of ln K_d versus $1/T$ (Figure 11).

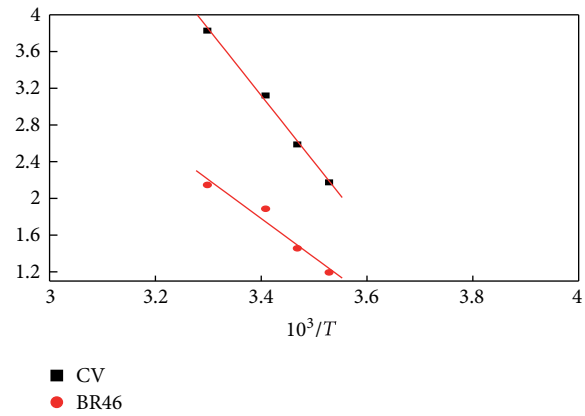

Figure 11: Arrhenius plots for the adsorption of CV and BR46 on to *P. Mutilus* at various temperatures.

The ΔH° and ΔS° values are positive. Based on the results of intra-particle model, this study proposed that the adsorption involved intra-particle diffusion that was not the only rate-controlling step and the other kinetic models might control the adsorption rate [39]. The positive value of entropy change (ΔS°) reflects good affinity of both dyes towards the sorbent and the increasing randomness at the solid-solution interface during the adsorption process [37].

The ΔG° value decreases from −5.10 to −9.62 kJ/mol and from −2.79 to −5.39 kJ/mol for CV and BR46, respectively, when the temperature increases from 10 to 30°C (Table 3), suggesting the more adsorbable of both dyes with increasing temperature. It was found from the values estimated for ΔG° that the spontaneity of adsorption of CV was greater than that of BR46. The values of ΔH° estimated for the adsorption of CV and BR46 were positive (Table 3). Thus, the adsorption reactions were endothermic, and that for the CV was greater than the BR46. The value of ΔH° estimated was >40 kJ·/mol for CV (59.60 Kj/mol) biosorption with *P. M,* indicating chemisorption nature of the reactions.

3.4. Biosorption in Binary Systems

3.4.1. Biosorption Selectivity in Binary Systems. Figure 12 shows a comparison of CV and BR46 adsorption on *P. M.* in binary systems at 0.6 g/L *P. M.*, 30°C and initial dye concentration of 10 mg/L. It is seen that CV and BR46 adsorption is reduced in binary system, which suggests a competitive adsorption. During the adsorption process, CV and BR46 adsorption are gradually increased and reached an equilibrium adsorption of 14 and 9,2 mg/g at 80 min, respectively, and compared with the adsorption rate in single system, CV and BR46 adsorption in binary system is slightly slower. The kinetics of CV and BR46 competitive adsorption in binary system was also studied using the above two models. Figures S10 and S11 illustrate the comparative results, and Table 2 lists the adsorption equilibrium and rate constants.

Table 2: Parameters of Pseudo-second-order and Weber-Morris model for biosorption of CV and BR46 onto *P. Mutilus* in single and binary system.

	Single system						
	K_2 (g·/mg/min)	q_e (mg/g)	h (mg/g·min)	r^2	k_i (g/mg·min$^{0.5}$)	r^2	D_i (cm^2/s)
			CV				
C_i (mg/L)							
10	7.39×10^{-2}	16.13	18.67	0.999	0.522	0.889.	3.29×10^{-8}
25	2.05×10^{-2}	38.46	30.30	0.997	1.66	0.943	2.21×10^{-8}
50	0.93×10^{-2}	76.92	55.55	0.998	2.37	0.916	2.03×10^{-8}
120	0.82×10^{-2}	142.85	166.66	0.998	4.31	0.852	3.28×10^{-8}
T (°C)							
10	7.2×10^{-2}	13.89	11.9	0.999	0.394	0.818	2.81×10^{-8}
15	5.18×10^{-2}	15.15	13.8	0.999	0.460	0.900	2.21×10^{-8}
20	8.12×10^{-2}	15.38	19.2	0.999	0.377	0.830	3.51×10^{-8}
30	7.39×10^{-2}	16.13	19.23	0.999	0.522	0.889	3.29×10^{-8}
			BR46				
C_i (mg/L)							
10	7.91×10^{-2}	12.05	11.49	0.999	0.376	0.865	2.89×10^{-8}
25	2.59×10^{-2}	20.83	11.23	0.999	0.88	0.874	1.51×10^{-8}
50	0.92×10^{-2}	40.00	14.7	0.998	1.94	0.931	1.03×10^{-8}
120	0.95×10^{-2}	52.63	26.31	0.999	3.35	0.917	3.4×10^{-8}
T (°C)							
10	6.34×10^{-2}	11.36	8.19	0.999	0.502	0.815	2.03×10^{-8}
15	6.45×10^{-2}	11.76	8.92	0.999	0.424	0.882	2.13×10^{-8}
20	7.58×10^{-2}	11.9	10.75	0.999	0.401	0.874	2.54×10^{-8}
30	7.91×10^{-2}	12.05	11.49	0.999	0.376	0.865	2.89×10^{-8}
	Binary system ($C_{iCV} = C_{iBR46} = 10$ mg/L, $T = 30$°C, pH = 7.5)						
	K_2 (g·/mg/min)	q_e (mg/g)	h (mg/g·min)	r^2	k_i (g/mg·min$^{0.5}$)	r^2	D_i (cm^2/s)
CV	6.50×10^{-2}	13.69	12.19	0.998	0.376	0.889.	2.5×10^{-8}
BR46	2.93×10^{-2}	8.93	2.34	0.994	0.640	0.930	0.74×10^{-8}

Table 3: Thermodynamic parameters.

Temperatures (°C)	$-\Delta G$ (kJ/mol)	$T\Delta S$ (kJ/mol)	ΔH (kJ/mol)
	CV		
10	5.10	2.29	59.60
15	6.18	3.43	
20	7.58	4.57	
30	9.62	6.86	
	BR46		
10	2. 79	0.5	34.75
15	3.47	0.75	
20	4.58	1	
30	5.39	1.5	

From Table 2, it is seen that the second-order kinetic shows close approximation to the experimental data, and the regression coefficients are much closer to each other. Based on the adsorption equilibrium, the individual adsorption of CV and BR46 is reduced by 15 and 26%, respectively. However, the total adsorption of natural *P. M.* is higher than that of any CV and BR46 equilibrium adsorption in single-component system. Table 2 shows that the diffusion coefficient is reduced by 24 and 74% for CV and BR46, respectively. The higher adsorption rate of CV than BR46 in binary system is due to the difference in structure and molecular size.

The relative adsorptions of CV and BR46 on *P. M.* in binary system were calculated from (9) [39]

$$a_r = \frac{[q_t]_B}{[q_t]_S}, \tag{9}$$

where $[q_t]_B$ and $[q_t]_S$ are the amount of adsorption of specific adsorbate in binary system and single system at time *t,* respectively. Also for the binary system, selectivity of adsorption on *P. M.* is defined as

$$S = \frac{[a_r]_{\text{CV}}}{[a_r]\,\text{BR46}}. \tag{10}$$

Figure 13 shows the variation of relative adsorption of CV and BR46 and the adsorption selectivity in binary system

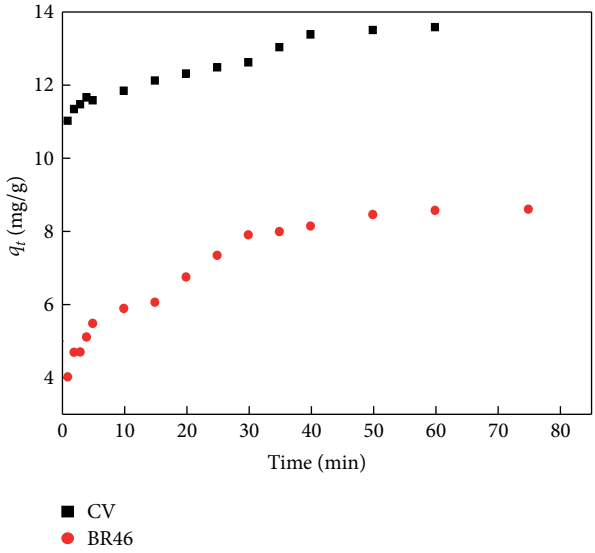

Figure 12: Biosorption kinetics in binary systems for CV and BR46.

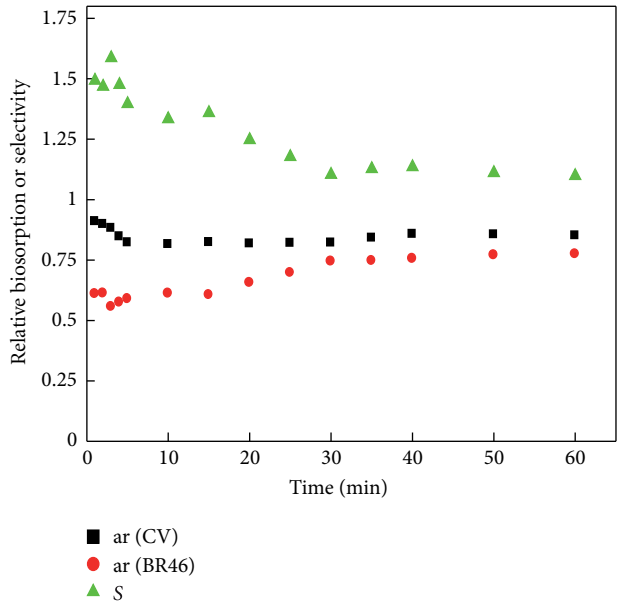

Figure 13: Relative biosorption and biosorption selectivity for CV and BR46 in binary system.

with time. It is seen that BR46 relative adsorption is gradually increased. This suggests that the presence of CV in solution does significantly influence the dynamic uptake process of BR46. The selectivity of adsorption shows a decreasing trend and approaches a constant value of 1.

This suggests that *P. M* has a higher affinity to CV biosorption in binary system, and the biosorption favors to the CV at initial stage. When the adsorption approaches the equilibrium, the adsorption selectivity will be the same for CV and BR46, the adsorption results suggest that the presence

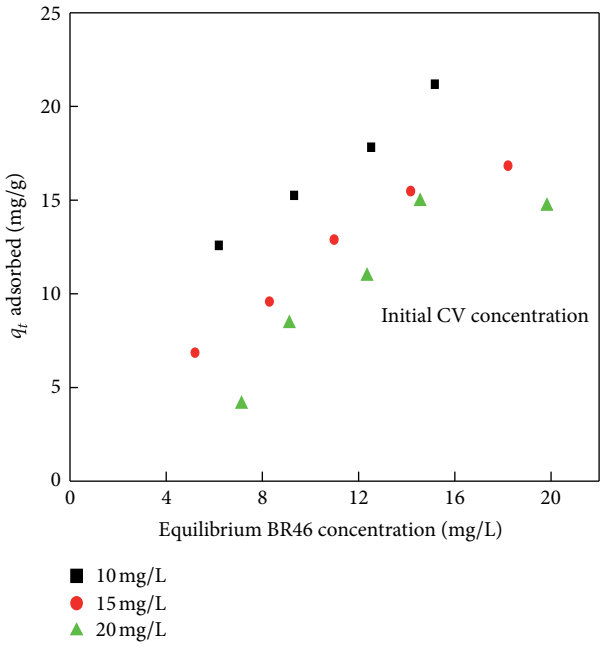

Figure 14: Biosorption isotherm of BR46 in the presence of CV.

of CV has significant influence on BR46 adsorption capacity, while CV adsorption including capacity and kinetics is affected by the presence of BR46.

3.4.2. Effect of Initial Dye Concentration on the Biosorption of BR46 and CV in Binary System. To investigate the effect of initial dye concentration on binary biosorption, experiments were divided into two stages. In the first part, $C_{i\,\mathrm{BR46}}$ was changed from 10 to 30 mg/L while $C_{i\,\mathrm{CV}}$ was at 10, 15, and 20 mg/L at pH value of 7.5 and biosorbent dosage of 0.6 g/L. In the second part, $C_{i\,\mathrm{CV}}$ was changed and $C_{i\,\mathrm{BR46}}$ was held at the same concentration range.

Biosorption Isotherm Models and Competitive Analysis in Binary Systems. Figure 14 shows the biosorption isotherm of BR46 by *P. M.* with varied concentration of CV. It is seen that the adsorption capacity of BR46 decreased with increasing concentration of CV. The biosorption of CV also reduced in the presence of BR46 (Figure 15); however, the degree of suppression was less than that of CV in BR46.

Various researchers have developed models in binary systems. In this study, the model chosen refers to theories developed by Sheindrof at al. (1981) derived a Freundlich-type multicomponent adsorption isotherm. The sheindorf-Rebhun-Sheintuch (SRS) equation was based on assumption that there is an exponential distribution of adsorption energies available for each solute [40]. A general SRS equation can be written as

$$(q_e)_i^j = K_{fi} C_{ei} \left(\sum a_{ij} C_{ej} \right)^{[(1/n_i)-1]}, \tag{11}$$

where $(q_e)_i^j$ is the amount of solute I adsorbed per unit weight of adsorbent in the presence of solute j. K_{fi} is the

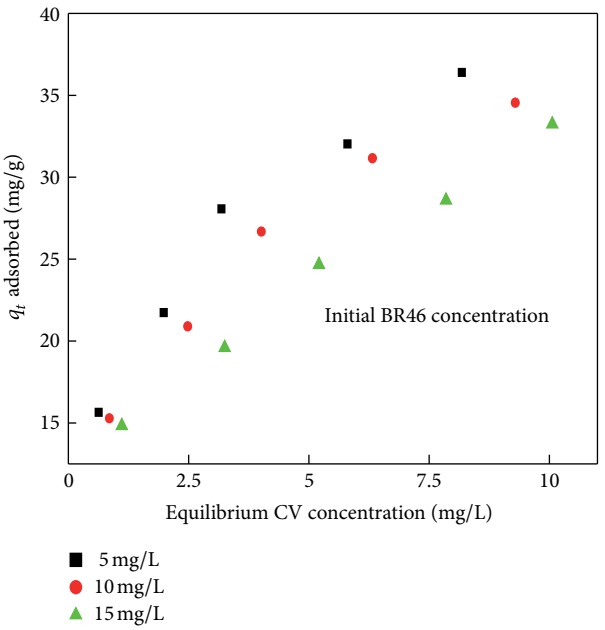

Figure 15: Biosorption isotherm of CV in the presence of BR46.

single-component Freundlich constant for solute i. $1/n$ is the Freundlich exponential term for solute i. C_{ei} and C_{ej} are the equilibrium concentrations of solute I and j, respectively and a_{ij} is the competitive coefficient. The bicomponent isotherm can be written [41, 42] as followas:

$$(q_e)_i^j = K_{fi} C_{ei} \left[C_{ei} + a_{ij} C_{ej} \right]^{[(1/n_i)-1]}. \quad (12)$$

In order to represent the batch isothermal data, the following linear forms of the SRS equation for binary solute system are used:

$$\frac{C_1}{C_2} = \left[\frac{\beta_1}{C_2} \right] - a_{12},$$
$$\frac{C_2}{C_1} = \left[\frac{\beta_2}{C_1} \right] - a_{21} \quad (13)$$

with

$$\beta_1 = \left(\frac{K_{F1} C_1}{q_1} \right)^{n_1/(n_1-1)}, \quad \beta_2 = \left(\frac{K_{F2} C_2}{q_2} \right)^{n_2/(n_2-1)}. \quad (14)$$

If both concentrations vary during the experiments, then plotting C_1/C_2 versus β_1/C_2 yields a straight line-of-unity slope and the competition coefficients (a_{12} and a_{21}) could be determined from the intercept (Figures 16(a) and 16(b)). The values of competitive coefficients a_{12} and a_{21} are 0.151 and 6.13, respectively. The magnitude of CV competition on BR46 adsorption by *P. M.* was significant. Parametric value of competition coefficient a_{21} for BR46 was 40 times higher than that observed for CV. The correlation coefficients (r^2) were found to be in the range of 0.951–0.983, which indicate a good relationship with the experimental data.

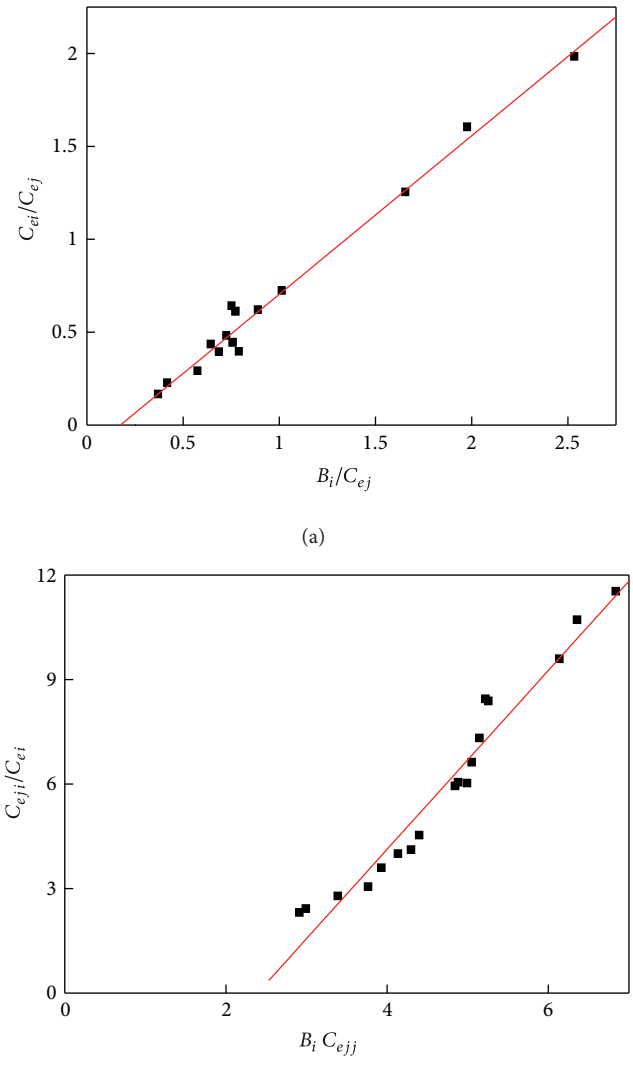

Figure 16: SRS competitive isotherm plots for (a) CV biosorption in the presence of BR46 and (b) BR46 biosorption in the presence of CV.

4. Conclusion

The present study shows that the *P. Mutilus* is an effective biosorbent for the removal of Crystal violet (CV) and Basic Red 46 (BR46) ions from aqueous solution. Maximum biosorption for CV and BR46 was found to occur at pH 7.5 and 8.1, respectively. The adsorption uptake of both dyes was very fast during the initial sorption period of about 5 min. Large adsorption capacity is registered for CV (q_{max} =166.66 mg/g), confirming its higher affinity for the biosorbent.

In single system, the Freundlich isotherm model yielded the concentration range. Batch studies show that a simple model of pseudo-second-order kinetic equation can adequately predict the adsorption of BR46 and CV on dead *P. mutilus* and the values of K_2, h, and q_e all increased with

the temperature, suggesting that increasing the temperature increased the adsorption capacity and the adsorption rate. These results imply that chemisorption mechanism may play an important role for the adsorption of BR46 and CV on the dead *P. mutilus*. Also, it was observed that the intraparticle diffusion was not the only rate controlling step. The kinetic parameter values obtained (*Di*) are of the same order of magnitude as those measured by other authors [43]. The thermodynamic study indicates that the adsorption of CV and BR46 onto *P. mutilus* is spontaneous and endothermic process.

In this study, the ability of *P. mutilus* to bind two basic dyes, BR46 and CV simultaneously in solution was investigated and the results were compared. The combined effects of two dyes on a biosorbent may be antagonistic. Since the initial biosorption rates and equilibrium dye removal decreased with increasing concentration of the other dye. In the binary dye mixtures, the affinity of the *P. Mutilis* for CV was greater than that for BR46. The proposed SRS equation is successfully employed to describe competitive adsorption data in the range of concentrations studied.

References

[1] S. Chowdhury, R. Mishra, P. Saha, and P. Kushwaha, "Adsorption thermodynamics, kinetics and isosteric heat of adsorption of malachite green onto chemically modified rice husk," *Desalination*, vol. 265, no. 1–3, pp. 159–168, 2011.

[2] F. Batzias, D. Sidiras, E. Schroeder, and C. Weber, "Simulation of dye adsorption on hydrolyzed wheat straw in batch and fixed-bed systems," *Chemical Engineering Journal*, vol. 148, no. 2-3, pp. 459–472, 2009.

[3] Y. Fu and T. Viraraghavan, "Removal of Congo Red from an aqueous solution by fungus *Aspergillus niger*," *Advances in Environmental Research*, vol. 7, no. 1, pp. 239–247, 2002.

[4] X.-J. Xiong, X.-J. Meng, and T.-L. Zheng, "Biosorption of C.I. Direct Blue 199 from aqueous solution by nonviable *Aspergillus niger*," *Journal of Hazardous Materials*, vol. 175, no. 1–3, pp. 241–246, 2010.

[5] V. K. Gupta, A. Rastogi, V. K. Saini, and N. Jain, "Biosorption of copper(II) from aqueous solutions by *Spirogyra* species," *Journal of Colloid and Interface Science*, vol. 296, no. 1, pp. 59–63, 2006.

[6] V. K. Gupta and A. Rastogi, "Biosorption of lead(II) from aqueous solutions by non-living algal biomass *Oedogonium* sp. and *Nostoc* sp.—a comparative study," *Colloids and Surfaces B*, vol. 64, no. 2, pp. 170–178, 2008.

[7] V. K. Gupta and A. Rastogi, "Sorption and desorption studies of chromium(VI) from nonviable cyanobacterium *Nostoc muscorum* biomass," *Journal of Hazardous Materials*, vol. 154, no. 1–3, pp. 347–354, 2008.

[8] V. K. Gupta and A. Rastogi, "Equilibrium and kinetic modelling of cadmium(II) biosorption by nonliving algal biomass *Oedogonium* sp. from aqueous phase," *Journal of Hazardous Materials*, vol. 153, no. 1-2, pp. 759–766, 2008.

[9] V. K. Gupta and A. Rastogi, "Biosorption of hexavalent chromium by raw and acid-treated green alga *Oedogonium hatei* from aqueous solutions," *Journal of Hazardous Materials*, vol. 163, no. 1, pp. 396–402, 2009.

[10] R. Pratibha, P. Malar, T. Rajapriya, S. Balapoornima, and V. Ponnusami, "Statistical and equilibrium studies on enhancing biosorption capacity of *Saccharomyces cerevisiae* through acid treatment," *Desalination*, vol. 264, no. 1-2, pp. 102–107, 2010.

[11] V. K. Gupta and I. Ali, "Removal of endosulfan and methoxychlor from water on carbon slurry," *Environmental Science and Technology*, vol. 42, no. 3, pp. 766–770, 2008.

[12] V. K. Gupta, B. Gupta, A. Rastogi, S. Agarwal, and A. Nayak, "Pesticides removal from waste water by activated carbon prepared from waste rubber tire," *Water Research*, vol. 45, no. 13, pp. 4047–4055, 2011.

[13] I. Ali and V. K. Gupta, "Advances in water treatment by adsorption technology," *Nature Protocols*, vol. 1, no. 6, pp. 2661–2667, 2007.

[14] W. W. Sung, B. C. Sun, and Y. S. Yun, "Interaction between protonated waste biomass of *Corynebacterium glutamicum* and anionic dye Reactive Red 4," *Colloids and Surfaces A*, vol. 262, no. 1–3, pp. 175–180, 2005.

[15] V. K. Gupta, I. Ali, and V. K. Saini, "Adsorption studies on the removal of Vertigo Blue 49 and Orange DNA13 from aqueous solutions using carbon slurry developed from a waste material," *Journal of Colloid and Interface Science*, vol. 315, no. 1, pp. 87–93, 2007.

[16] V. K. Gupta, A. Mittal, V. Gajbe, and J. Mittal, "Removal and recovery of the hazardous azo dye acid orange 7 through adsorption over waste materials: bottom ash and de-oiled soya," *Industrial and Engineering Chemistry Research*, vol. 45, no. 4, pp. 1446–1453, 2006.

[17] S. T. Akar, A. Gorgulu, T. Akar, and S. Celik, "Decolorization of Reactive Blue 49 contaminated solutions by *Capsicum annuum* seeds: batch and continuous mode biosorption applications," *Chemical Engineering Journal*, vol. 168, no. 1, pp. 125–133, 2011.

[18] Z. Aksu and A. B. Akin, "Comparison of Remazol Black B biosorptive properties of live and treated activated sludge," *Chemical Engineering Journal*, vol. 165, no. 1, pp. 184–193, 2010.

[19] Y. Yang, G. Wang, B. Wang et al., "Biosorption of Acid Black 172 and Congo Red from aqueous solution by nonviable *Penicillium* YW 01: kinetic study, equilibrium isotherm and artificial neural network modeling," *Bioresource Technology*, vol. 102, no. 2, pp. 828–834, 2011.

[20] C.-Y. Tan, M. Li, Y.-M. Lin, X. Q. Lu, and Z. L. Chen, "Biosorption of Basic Orange from aqueous solution onto dried *A. filiculoides* biomass: equilibrium, kinetic and FTIR studies," *Desalination*, vol. 266, no. 1–3, pp. 56–62, 2011.

[21] D. Charumathi and N. Das, "Packed bed column studies for the removal of synthetic dyes from textile wastewater using immobilised dead *C. tropicalis*," *Desalination*, vol. 285, no. 31, pp. 22–30, 2012.

[22] N. Yeddou-Mezenner, "Kinetics and mechanism of dye biosorption onto an untreated antibiotic waste," *Desalination*, vol. 262, no. 1–3, pp. 251–259, 2010.

[23] A. Mittal, J. Mittal, A. Malviya, D. Kaur, and V. K. Gupta, "Adsorption of hazardous dye crystal violet from wastewater by waste materials," *Journal of Colloid and Interface Science*, vol. 343, no. 2, pp. 463–473, 2010.

[24] S. Senthilkumaar, P. Kalaamani, and C. V. Subburaam, "Liquid phase adsorption of Crystal Violet onto activated carbons derived from male flowers of coconut tree," *Journal of Hazardous Materials*, vol. 136, no. 3, pp. 800–808, 2006.

[25] Y. S. Ho, "Review of second-order models for adsorption systems," *Journal of Hazardous Materials*, vol. 136, no. 3, pp. 681–689, 2006.

[26] W. J. Weber and J. C. Morris, "Kinetics of adsorption on carbon from solution," *Journal of the Sanitary Engineering Division. Proceedings. American Society of Civil Engineers*, vol. 89, pp. 31–60, 1963.

[27] G. McKay and V. J. P. Poots, "Kinetics and diffusion processes in colour removal from effluent using wood as an adsorbent," *Journal of Chemical Technology and Biotechnology*, vol. 30, no. 6, pp. 279–292, 1980.

[28] L. D. Michelsen, P. G. Gideon, E. G. Pace, and L. H. Kutsal, "Removal of soluble mercury from waste water by complexing techniques," Bulletin no. 74, US Department of Industry. Office of the Water Research and Technology, 1975.

[29] B. Cheknane, O. Bouras, M. Baudu, J. P. Basly, and A. Cherguielaine, "Granular inorgano-organo pillared clays (GIOCs): preparation by wet granulation, characterization and application to the removal of a Basic dye (BY28) from aqueous solutions," *Chemical Engineering Journal*, vol. 158, no. 3, pp. 528–534, 2010.

[30] J. M. Deacon, *Fungal Biology*, Blackwell Publishing, 4th edition, 2006.

[31] C. Namasivayam and S. Sumithra, "Removal of direct Red 12B and methylene blue from water by adsorption onto Fe (III)/Cr (III) hydroxide, an industrial solid waste," *Journal of Environmental Management*, vol. 74, no. 3, pp. 207–215, 2005.

[32] S. Debnath and U. C. Ghosh, "Equilibrium modeling of single and binary adsorption of Cd(II) and Cu(II) onto agglomerated nano structured titanium(IV) oxide," *Desalination*, vol. 273, no. 2-3, pp. 330–342, 2011.

[33] I. Langmuir, "The adsorption of gases on plane surfaces of glass, mica and platinum," *The Journal of the American Chemical Society*, vol. 40, no. 9, pp. 1361–1368, 1918.

[34] H. Freundlich, "Adsorption in solution," *Journal of Physical Chemistry*, vol. 40, pp. 1361–1368, 1906.

[35] M. Arami, N. Y. Limaee, and N. M. Mahmoodi, "Evaluation of the adsorption kinetics and equilibrium for the potential removal of acid dyes using a biosorbent," *Chemical Engineering Journal*, vol. 139, no. 1, pp. 2–10, 2008.

[36] F. Deniz and S. D. Saygideger, "Removal of a hazardous azo dye (Basic Red 46) from aqueous solution by princess tree leaf," *Desalination*, vol. 268, no. 1–3, pp. 6–11, 2011.

[37] N. Y. Mezenner and A. Bensmaili, "Kinetics and thermodynamic study of phosphate adsorption on iron hydroxide-eggshell waste," *Chemical Engineering Journal*, vol. 147, no. 2-3, pp. 87–95, 2009.

[38] B. H. Hameed, A. A. Ahmad, and N. Aziz, "Isotherms, kinetics and thermodynamics of acid dye adsorption on activated palm ash," *Chemical Engineering Journal*, vol. 133, no. 1–3, pp. 195–203, 2007.

[39] S. Wang and E. Ariyanto, "Competitive adsorption of malachite green and Pb ions on natural zeolite," *Journal of Colloid and Interface Science*, vol. 314, no. 1, pp. 25–31, 2007.

[40] C. Sheindorf, M. Rebhun, and M. Sheintuch, "A Freundlich-type multicomponent isotherm," *Journal of Colloid And Interface Science*, vol. 79, no. 1, pp. 136–142, 1981.

[41] C.-H. Wu, C. Y. Kuo, C.-F. Lin, and S.-L. Lo, "Modeling competitive adsorption of molybdate, sulfate, selenate, and selenite using a Freundlich-type multi-component isotherm," *Chemosphere*, vol. 47, no. 3, pp. 283–292, 2002.

[42] V. P. Vinod and T. S. Anirudhan, "Adsorption behaviour of basic dyes on the humic acid immobilized pillared clay," *Water, Air, and Soil Pollution*, vol. 150, no. 1–4, pp. 193–217, 2003.

[43] D. Chatzopoulos, A. Varma, and R. L. Irvine, "Activated carbon adsorption and desorption of toluene in the aqueous phase," *AIChE Journal*, vol. 39, no. 12, pp. 2027–2041, 1993.